Nationaal Lucht- en Ruimtevaartlaboratorium
National Aerospace Laboratory NLR

NLR-TP-2000-384

Fatigue and corrosion in aircraft pressure cabin lap splices

R.J.H. Wanhill and M.F.J. Koolloos

Nationaal Lucht- en Ruimtevaartlaboratorium
National Aerospace Laboratory NLR

NLR-TP-2000-384

Fatigue and corrosion in aircraft pressure cabin lap splices

R.J.H. Wanhill and M.F.J. Koolloos

This report is based on an article to be published in a special issue of the International Journal of Fatigue.

Division:	Structures and Materials
Issued:	19 July 2000
Classification of title:	Unclassified

Contents

(30 pages in total)

This page is intentionally left blank.

FATIGUE AND CORROSION IN AIRCRAFT PRESSURE CABIN LAP SPLICES

R.J.H. Wanhill* and M.F.J. Koolloos

National Aerospace Laboratory NLR, P.O. Box 90502
NL-1006 BM Amsterdam, The Netherlands

Aircraft structures are susceptible to fatigue and corrosion damage, notably at joints. There may be interactions between fatigue and corrosion, especially as aircraft age. Longitudinal lap splices from several types of transport aircraft pressure cabins were disassembled and investigated for Multiple Site Damage (MSD) fatigue cracking and corrosion. The results are compared with NASA data for a full-scale fatigue test. Broadly speaking, pressure cabin lap splices have either a fatigue problem or a corrosion problem: MSD fatigue cracking is not initiated by corrosion. The results are discussed with respect to lap splice MSD fatigue modelling, testing and analysis.

(Keywords: fatigue, corrosion, aircraft pressure cabins)

INTRODUCTION

NASA [1], Fokker [2] and the NLR have obtained fractographic data on Multiple Site Damage (MSD) fatigue cracking in longitudinal lap splices of transport aircraft pressure cabins. These data are supplemented by IAR [3] and NLR examination of severely corroded lap splices. The lap splices came from five service aircraft, namely three Fokker F28s, a British Aerospace BAC 1-11 and a Boeing 727-100, and full-scale tests on a Fokker 100 and the forward fuselage of a Boeing 747-400 [4]. The histories of all seven pressure cabins are summarised in table 1.
This paper covers the results so far, considering (1) MSD fatigue crack initiation and early crack growth, (2) corrosion and any associations between corrosion and MSD, and (3) the consequences for lap splice MSD fatigue modelling and analysis.

LAP SPLICE POSITIONS AND CONFIGURATIONS

Figures 1-3 show the positions of the investigated lap splices, specifying the predominant damage, MSD fatigue cracks or corrosion. Figure 4 shows the configurations of the lap splices investigated by the NLR. The positions and configurations differed widely, and the B 747-400 lap splice was different again: a four rivet row design with a Z-stiffener along the lower inner

* Corresponding author. Fax: 00-31-52724-8210. e-mail: wanhill@nlr.nl

row [1]. The single common feature of all the lap splices was the sheet material, aluminium alloy 2024-T3 Alclad.

FATIGUE

Fatigue assessment was to determine the MSD locations, any environmental (corrosion) influences on fatigue crack initiation and growth, the crack initiation lives and early crack growth rates. As expected [5], the most MSD-susceptible rivet row was the upper one in the outer sheet of each lap splice. However, other rivet rows were also susceptible, notably the lower one in the inner sheet, see figure 1 and Piascik and Willard [1].

MSD fatigue initiation characteristics
Figure 5 shows the characteristic MSD fatigue crack locations and shapes. These are discussed next, followed by a summary:

(1) F28-4000 service aircraft: The total lengths of MSD were 530 mm and 330 mm for aircraft (1) and (2) respectively. The cracks initiated at many sites along the faying surface edges of the outer sheet dimpling cones, see figures 4 and 5. The cracks were mechanically induced, with no evidence that corrosion aided initiation. The large number of initiation sites suggests that fatigue cracking began soon after the aircraft entered service.

(2) BAC 1-11 service aircraft: MSD was along about 500 mm of port and starboard lap splices. The cracks initiated at a variety of locations, see figure 5, though mainly at faying surfaces close to the rivet holes (types A, C and D). There was no evidence that corrosion aided initiation.

(3) F100 full-scale test (indoors): MSD extended over several frame bays having poor adhesive bonds. The cracks initiated from the faying surfaces, mostly at multiple sites close to the rivet holes, see figure 5. There was no evidence of corrosion, as expected from a test indoors.

(4) B 747-400 full-scale test (outdoors): MSD extended over several frame bays, see figure 2. The cracks initiated at a variety of locations, see figure 5, though mainly at faying surfaces (types A, A´) and rivet hole/faying surface corners (types C, D) [1]. There was no evidence of corrosion, even though the test was outdoors.

In summary, bearing in mind that the F28 dimpled lap splices are uncustomary, the in-service and full-scale test MSD fatigue initiation occurred mostly from faying surfaces near or at the rivet hole corners . This means that the faying surface condition (cladding, anodising, priming, interfay sealant, adhesive bonding) and rivet hole corner quality are important. Also, fretting must play a role, if not always during crack initiation, then probably during early crack growth [6].

Secondary fatigue initiation characteristics: B 727-100 aircraft

Secondary fatigue cracks in the B 727-100 lap splice usually initiated from intergranular corrosion cracking (exfoliation corrosion and stress corrosion) which had already spread away from the rivet positions. However, twelve small fatigue cracks were found at six rivet hole positions, without any evidence of fatigue initiation due to local corrosion (pitting), for example figure 6. Figure 7 shows the locations and shapes of these fatigue cracks at the rivet holes. Ten of the cracks occurred inside the rivet holes in the inner sheet. This behaviour is distinct from MSD, where the majority of cracks initiated from faying surfaces, and is discussed later in the paper.

Early fatigue crack growth: environmental effects

Unlike fatigue initiation, there was evidence of (local) environments affecting the service aircraft fatigue fracture surfaces, either by post-cracking corrosion or during crack growth. The MSD and secondary fatigue fracture surfaces from the F28-4000, BAC 1-11 and B 727-100 service aircraft showed some post-cracking corrosion, making it difficult to measure fatigue striation spacings near the crack initiation sites. However, this post-cracking corrosion was generally mild, since otherwise the fatigue fracture surfaces would have been obliterated [7].
Of more interest are environmental effects during fatigue crack growth. Evidence for such effects was observed:

(1) Figure 8 shows a particularly clear example of fracture surface “beach marks”. These sometimes occurred during early MSD crack growth in the F28-4000 and BAC 1-11 lap splices, and were usually present on the secondary fatigue fracture surfaces from the B 727-100 lap splice. The beach marks may indicate periodic changes in the local environment [8, 9]. At least for the F28-4000 aircraft, it is certain that the beach marks were not due to variable amplitude loading, since the pressure cabins of these aircraft experienced the maximum pressure differential in each flight.

(2) Figure 9 shows a secondary fatigue fracture surface from the B 727-100 lap splice, with special features (arrowed) similar to those found - albeit more abundantly - for corrosion fatigue at low stress intensities [7].

Presently the significance of these observations, other than being diagnostic for environmental fatigue crack growth, is limited. Fatigue striation spacing measurements for the light and dark bands comprising the beach marks have not shown systematic differences in crack growth rates. This could mean that modelling and prediction of early MSD crack growth need not account for environmental effects beyond that of normal air, but more work needs to be done, notably tests at low cycle frequencies of the same order as in-service cabin pressure cycling, and at overall crack growth rates similar to those for early MSD crack growth in the lap splices.

Early MSD crack growth rates

(1) Transverse (through-thickness): observation of transverse fatigue crack growth near the rivet holes was often hampered by fretting products and, for service aircraft, fracture surface corrosion. Figure 10 summarises the data obtainable from fatigue striation measurements on fracture surfaces from the F28-4000 and BAC 1-11 service aircraft and the F100 full-scale test. Also shown is an estimate for the F100 test at 100 % design load. This estimate is derived from the factor $(100/110)^{7.1}$, where 7.1 is the "Paris Law" exponent in a piecewise linear fit to log da/dN versus log ΔK data for 2024-T3 in the same range of crack growth rates [10].

Figure 10 shows two noteworthy features: (a) through-thickness crack growth rates were more or less constant for each aircraft type, and (b) the data and estimate indicate crack growth rates all above 10^{-8} m/cycle.

(2) Longitudinal: figure 11 summarises the data obtained from fatigue striation and marker band measurements for the BAC 1-11, F100 and B 747-400 aircraft, together with an estimate for the F100 test at 100 % design load, as discussed above. The BAC 1-11 and F100 data are presented more fully in [2, 10], and the BAC 1-11 lap splices are still being investigated.

As before, the data and estimate indicate crack growth rates above 10^{-8} m/cycle. Also, the crack growth rates for different aircraft types were fairly similar in the range of crack sizes 0.5 mm – 2 mm. This is remarkable in view of the differing lap splice configurations, see figure 4 and [1].

These features of early MSD crack growth will be returned to in the section on MSD fatigue modelling and testing.

CORROSION

The lap splice samples from severely corroded areas of the B 727-100 and F28-1000 service aircraft were examined for any cracking along the rivet rows and at or near the rivet holes.

B 727-100

The lap splice sample was provided by the IAR after non-destructive examination using D sight, eddy current and X-ray techniques [3]. Corrosion was visibly concentrated internally along the upper side of the lap splice/stiffener connection (R.H. side in figure 4), but D sight showed corrosion-induced "pillowing" to be present throughout the lap splice: corrosion-induced pillowing is bulging of the lap splice between the rivet positions, and is caused by local build-ups of corrosion products between the outer and inner sheets.

Figure 12 summarises the results of lap splice disassembly and examination by the NLR, combining the information from the outer and inner sheets. Almost 95 % of the cracking, in terms of crack locations, was intergranular owing to exfoliation corrosion and stress corrosion, the latter especially as corrosion built up between the sheets to cause locally high stresses [11]. Some of the larger intergranular cracks were associated with small, secondary fatigue cracks. These fatigue cracks usually initiated from intergranular cracking, but sometimes directly from rivet holes, as mentioned earlier in the paper with reference to figures 6 and 7. Also, figure 12 shows fatigue cracking at two rivet positions (96 and 99) that had not undergone intergranular cracking but were close to severe corrosion revealed by lap splice disassembly.

The secondary fatigue cracks at - and especially in - the rivet holes most probably initiated owing to a combination of normal in - service stresses and additional stresses caused by corrosion product build-ups between the outer and inner sheets.

F28-1000

The lap splice sample was a strip 165 cm long containing about 200 rivets. The sample had been removed from the position shown in figure 3, owing to excessive externally visible corrosion. This had previously led to the lap splice outer sheet being "cleaned up" to a depth of about 0.25 mm, reducing the sheet thickness from 1.2 mm, figure 4, to less than 1mm.

Disassembly and detailed examination, including opening-up selected outer sheet rivet holes by tensile testing, showed no evidence of any pre-existing cracks. This result was unexpected, since the position of the sample was known to be MSD-susceptible. In fact, a 450 mm long MSD fatigue crack was found in the same aircraft at the same location on the left-hand side of the pressure cabin.

From these results we may draw two conclusions:

(1) Excessive external corrosion in an MSD-susceptible area need not be associated with fatigue cracking, despite stress increases in the lap splice outer sheet owing to cleaning up and thinning it.

(2) Even in an MSD-susceptible area it is possible to accumulate many flights (34,470 , see table 1) without fatigue crack initiation.

MSD FATIGUE MODELLING AND TESTING

General remarks

Fatigue of pressure cabin longitudinal lap splices is determined by locally complex stress distributions very difficult to determine [5, 10, 12]. In particular, this means realistic stress intensity factor solutions are unavailable for cracks smaller than the sheet thicknesses; and one may doubt the usefulness, through lack of accuracy, of solutions for cracks with dimensions less than the rivet hole diameters.

Nor does it seem possible to model fatigue initiation by stress analysis. This is not only because of the complex stress fields, but also because MSD fatigue initiation in lap splices depends strongly on the local behaviour of various materials (aluminium alloy matrix, cladding and anodised layers, primers and sealants) at the faying surfaces and near or at rivet hole corners [10, 13]. Note that models based on fatigue initiation at corrosion pits [14] or inclusions in the aluminium alloy matrix [15] are most probably inappropriate for 2024-T3 Alclad lap splices: the F28-4000 and BAC 1-11 service aircraft samples showed no evidence of corrosion pitting, and tests have shown fatigue cracks initiate in the cladding, not the 2024-T3 matrix [12, 16, 17].

Instead - at least for now - recourse must be made to empirical modelling that describes the *actual* early MSD fatigue behaviour of lap splices from service aircraft and full-scale tests. One such model, by Eijkhout [2], is described next.

Empirical model of early MSD fatigue behaviour

Eijkhout's model [2] is based on the following observations:

(1) MSD fatigue cracks tend to initiate at several sites near or at rivet hole corners, and grow in directions varying gradually from transverse (through-thickness) to longitudinal, see the F100 sketch in figure 5.

(2) The transverse crack growth rates are nearly constant, e.g. figure 10.

(3) The transverse and longitudinal crack growth rates are similar for cracks smaller than twice the sheet thickness, compare figure 10 with figure 11 for crack lengths up to about 2.5 mm (sheet thicknesses 1.2 – 1.25 mm, see figure 4).

Figure 13 is a schematic of the model. There are three main assumptions, the first two being derived from the foregoing observations: (a) constant crack growth rate in the transverse direction, generally equal to the initial crack growth rate in the longitudinal direction, i.e. $dc/dN = Ae^{Ba_i}$; (b) crack depth $c = 0$ at a_i , the "initiation length"; and (c) quarter-circular crack fronts in the transition from transverse to longitudinal crack growth. These assumptions are

convenient but not essential. For example, the model can be used for non-constant dc/dN and for crack initiation at rivet hole corners, i.e. $a_i = 0$ in figure 13. Also the model can be used for both non-countersunk and countersunk lap splice sheets [2].

Examples of the model's use are given in Eijkhout's report [2]. The model provides estimates of the fatigue crack growth lives and hence the fatigue "initiation" lives, N_i in figure 13, whereby N_i is taken to be the fatigue life beyond which there is a regular process of crack growth.
Two further aspects are of interest. Firstly, the model enables estimates of the lives at which MSD fatigue cracks become through-thickness, which information is potentially useful for in-service non-destructive inspection. Secondly, the model can be made compatible with marker bands on the fatigue fracture surfaces from full-scale tests, as in the case of the B 747-400 [1]: when determining the striation-based crack growth equations, $da/dN = Ae^{Ba}$, for individual cracks, one can check the equations' compatibility with the distances between marker bands, adjusting the equations as necessary.

MSD fatigue initiation lives
Table 2 gives estimates of the MSD fatigue initiation lives (lives to *first* crack initiation) for the F28-4000, F100, BAC 1-11 and B 747-400 aircraft types. The F28-4000 estimate is only a reasonable guess. The F100 and BAC 1-11 estimates were obtained with Eijkhout's model, described above. The B 747-400 estimates were made from marker band analyses [1].
There is considerable variation in the estimates, though the F28-4000 lap splices are not of general interest, and one would expect the shorter fatigue lives for B 747-type aircraft, which were designed for a service life of 20,000 flights [18]. Actually, the total variation in initiation lives for the F100 and BAC 1-11 aircraft is greater: for the F100 full-scale test the estimates ranged from 60,000 – 97,000 simulated flights, and for the BAC 1-11 the estimates ranged from 50,000 – 74,000 flights.

MSD fatigue crack growth behaviour and its significance for testing
From the information provided by figures 10 and 11 it is apparent that the transverse and longitudinal fatigue crack growth rates were above 10^{-8} m/cycle for crack sizes ranging from 30 μm to 5 mm. For 2024-T3 this means only long crack growth behaviour should be operative [10, 19], which facilitates crack growth modelling and agrees with Eijkhout's approach [2].
On the other hand, these relatively high early crack growth rates in actual pressure cabin longitudinal lap splices make questionable the usefulness and relevance of sub-scale specimen tests. Uniaxial specimens "simulating" the F100 pressure cabin longitudinal lap splices had early crack growth rates far too low compared to the full-scale test results [20]. This was also true for biaxial specimens [21]. This situation may change when improved stress analyses

become available and are used for improving sub-scale specimen design and testing. However, it may turn out that reliance will still have to be made mainly on full-scale tests [22, 23].

LAP SPLICE FATIGUE ANALYSES

Analysis methods

Figure 14 shows the "traditional" and developing fatigue analysis methods for transport aircraft pressure cabin lap splices. In the "traditional" methods the inspection threshold is established using fatigue life S-N data, cumulative linear damage analysis (if deemed necessary) and scatter factors. Subsequent inspection intervals are based on a safe fatigue crack growth period using da/dN versus ΔK_{eff} long crack growth data, crack growth models for spectrum loading (if deemed necessary) and scatter factors.

In the developing methods the inspection threshold is intended to be established using fatigue crack growth analysis and tests, whereby it is assumed the structure contains initial flaws (Initial Quality Flaw Sizes, IQFS). Subsequent inspection intervals are based on a safe fatigue crack growth period that accounts for MSD essentially as a refinement – however important – to the "traditional" analyses.

Analysis problems: actual versus predicted behaviour

Figure 15 is a schematic of the probable differences between actual early MSD crack growth behaviour and predictions using macroscopic (long) crack growth modelling, whereby the IQFS values are obtained either from actual data for manufacturing flaws or by back-extrapolation using a long crack growth model.

For both types of prediction the long crack growth model is used to make an empirical fit such that the fatigue life is represented as a regular crack growth process, beginning as soon as the aircraft enters service. This premise is incorrect: crack initiation is a physical reality, however uncertain its definition (as mentioned earlier, we take "initiation" to be the fatigue life beyond which there is a regular process of crack growth). The fitted model therefore has limited transferability, and in general should not be used for "blind" predictions of crack growth in other structural areas with differing lap splice geometries and – most importantly – differing faying surface conditions. Nor should the fitted model be used for predicting crack growth at different (local) stress levels. This latter point is significant for two reasons:

(1) The stress-dependence of fatigue initiation life will probably be very different to that of fatigue crack growth, e.g. [24].

(2) Actual fatigue crack growth rates could be in a different "Paris Law" regime, i.e. the exponent m in the relation $da/dN = C(\Delta K)^m$ could be different. An example of a surprisingly high but realistic exponent, m = 7.1, was mentioned earlier, with reference to figure 10.

There would seem to be no solution to the above problems so long as it is assumed that crack growth begins as soon as the aircraft enters service. One alternative is to further investigate the usefulness of Eijkhout's model. This possibility has much to recommend it. The model is based on physical reality: it takes account of actual lap splice MSD fatigue initiation and crack growth behaviour, and the present paper has shown much commonality in this behaviour for several aircraft types and different positions of the lap splices. Also, as mentioned earlier, it may turn out that MSD fatigue modelling will have to rely mainly on full-scale fatigue testing. If so, then Eijkhout's model provides a way of describing crack growth, notably the most important early crack growth through the sheet thickness, and a way of estimating the fatigue initiation life. Of course, since the model is empirical, the parameters in the model have to be determined for each type of aircraft, and also – possibly – for fuselage areas where the design stress levels are significantly different, e.g. varying by more than 10 % from the average.

CONCLUSIONS

The characteristics of MSD fatigue and corrosion in transport aircraft pressure cabin longitudinal lap splices have been investigated using samples from five service aircraft, namely three Fokker F28s, a British Aerospace BAC 1-11 and a Boeing 727-100, and full-scale test data for the Fokker 100 and the forward fuselage of a Boeing 747-400 [1]. The following conclusions are drawn:

(1) There is no *primary* association between MSD fatigue and corrosion for 2024-T3 Alclad lap splices. However, there was evidence of local environmental effects during early MSD fatigue crack growth in lap splices from service aircraft. It is uncertain whether the fatigue crack growth rates in service are significantly different, owing to environmental effects, from those determined by testing in laboratory air.

(2) There was a strong tendency for MSD fatigue cracks to initiate at faying surfaces near or at rivet hole corners. However, for the severely corroded B 727-100 lap splice secondary fatigue cracks initiated usually from intergranular cracks due to corrosion and stress corrosion, but sometimes occurred directly from rivet holes, albeit without any evidence of fatigue initiation due to local corrosion.

(3) A distinction should be made between MSD fatigue initiation and fatigue crack growth: it is physically incorrect to consider lap splice fatigue solely as a regular crack growth process that begins as soon as the aircraft enters service.

(4) There are indications of considerable variation in MSD fatigue initiation lives, both in the range of lives for each aircraft type and between aircraft types.

(5) The most MSD-susceptible rivet row was the upper one in the outer sheets of the lap splices. However, other rivet rows were susceptible, notably the lower one in the inner sheets.

(6) Early MSD fatigue crack growth rates, for crack sizes 30 μm – 5 mm, were above 10^{-8} m/cycle (or flight), which means one should not expect any difference between short and long fatigue crack behaviour in the lap splices. However, the relatively high crack growth rates make questionable the usefulness and relevance of sub-scale specimen tests.

The foregoing conclusions should be taken into account during further development of fatigue analysis methods for transport aircraft pressure cabin lap splices.

REFERENCES

(1) Piascik, R.S. and Willard, S.A., The characteristics of fatigue damage in the fuselage riveted lap splice joint, NASA Technical Publication NASA/TP-97-206257, National Aeronautics and Space Administration Langley Research Center, Hampton, Virginia, November 1997.

(2) Eijkhout, M.T., Fractographic analysis of longitudinal fuselage lapjoint at stringer 42 of Fokker 100 full scale test article TA15 after 126250 simulated flights, Fokker Report RT2160, Fokker Aircraft Ltd., Amsterdam, November 1994.

(3) Chapman, C.E. and Fahr, A., Nondestructive examination of aircraft lap joint specimens for the Netherlands National Aerospace Laboratory, Memorandum LM-ST-787, Institute for Aerospace Research, National Research Council Canada, Ottawa, February 1997.

(4) Gopinath, K.V., Structural airworthiness of aging Boeing jet transports – 747 fuselage fatigue test program, 1992 Aerospace Design Conference, AIAA 92-1128, American Institute of Aeronautics and Astronautics, Washington, D.C., February 1992.

(5) Eastaugh, G.F., Simpson, D.L., Straznicky, P.V. and Wakeman, R.B., A special uniaxial coupon test specimen for the simulation of multiple site fatigue crack growth and link-up in fuselage skin splices, Widespread Fatigue Damage in Military Aircraft, AGARD

Conference Proceedings 568, Advisory Group for Aerospace Research and Development, pp. 2-1 – 2-19, Neuilly-sur-Seine (1995).

(6) Rooke, D.P., Fracture mechanics analysis of short cracks at loaded holes, Behaviour of Short Cracks in Airframe Components, AGARD Conference Proceedings No. 328, Advisory Group for Aerospace Research and Development, pp. 8-1 – 8-6, Neuilly-sur-Seine (1983).

(7) Wanhill, R.J.H. and Schra, L., Corrosion fatigue crack arrest in aluminium alloys, Quantitative Methods in Fractography, ASTM STP 1085, Editors B.M. Strauss and S.K. Putatunda, American Society for Testing and Materials, pp. 144-165, Philadelphia, Pennsylvania (1990).

(8) Darvish, M. and Johansson, S., Cyclic change in the humidity of the environment during fatigue crack propagation and its effect on fracture surface appearance, Scandinavian Journal of Metallurgy, Vol. 21, pp. 68-77 (1992).

(9) Mussert, K.M., Formation of beach marks on Alclad 2024-T3 sheet, Master of Science Thesis, Department of Chemical Technology and Materials Science, Delft University of Technology, Delft, December 1995.

(10) Wanhill, R.J.H., Fractography of MSD in fuselage lap splices, Brite Euram Project No. BE95-1053, SMAAC: Structural Maintenance of Ageing Aircraft, Document No. SMAAC-TR-1.3-02-1.3/NLR, NLR Technical Report TR 98310, National Aerospace Laboratory, Amsterdam, July 1998.

(11) Komorowski, J.P., Bellinger, N.C. and Gould, R.W., The role of corrosion pillowing in NDI and in the structural integrity of fuselage joints, ICAF 97, Fatigue in New and Ageing Aircraft, Editors R. Cook and P. Poole, Engineering Materials Advisory Services Ltd., Vol. 1, pp. 251-266, Cradley Heath (1997).

(12) Müller, R.P.G., An experimental and analytical investigation on the fatigue behaviour of fuselage riveted lap joints, Delft University Press, Delft (1995).

(13) Wanhill, R.J.H., Effects of cladding and anodising on flight simulation fatigue of 2024-T3 and 7475-T761 aluminium alloys, NLR Technical Report TR 85006 L, National Aerospace Laboratory, Amsterdam, January 1985.

(14) Wei, R.P. and Harlow, D.G., Corrosion and corrosion fatigue of aluminium alloys – an aging aircraft issue, Fatigue ’99, Proceedings of the Seventh International Fatigue Congress, Editors Xue-Ren Wu and Zhong-Guang Wang, Engineering Materials Advisory Services Ltd., Vol. 4, pp. 2197-2204, Cradley Heath (1999).

(15) Laz, P.J., Craig, B.A., Rohrbaugh, S.M. and Hillberry, B.M., The development of a total fatigue life approach accounting for nucleation and propagation, Fatigue ’99, Proceedings of the Seventh International Fatigue Congress, Editors Xue-Ren Wu and Zhong-Guang Wang, Engineering Materials Advisory Services Ltd., Vol. 2, pp. 833-838, Cradley Heath (1999).

(16) Forsyth, P.J.E., The effect of cladding condition on the stages of fatigue crack formation and growth, Problems with Fatigue in Aircraft, Proceedings of the Eighth ICAF Symposium, Editors J. Branger and F. Berger, Swiss Federal Aircraft Establishment (F+W), pp. 2.5/1 – 2.5/23, Emmen (1975).

(17) Schijve, J., Jacobs, F.A. and Tromp, P.J., The significance of cladding for fatigue of aluminium alloys in aircraft structures, NLR Technical Report TR 76065 U, National Aerospace Laboratory, Amsterdam, July 1976.

(18) Spencer, M.M., The Boeing 747 fatigue integrity program, Advanced Approaches to Fatigue Evaluation, Proceedings of the Sixth ICAF Symposium, NASA SP-309, National Aeronautics and Space Administration, pp. 127-178, Washington, D.C. (1972).

(19) Newman, Jr., J.C. and Edwards, P.R., Short-crack growth behaviour in an aluminium alloy – an AGARD Cooperative Test Programme, AGARD Report No. 732, Advisory Group for Aerospace Research and Development, Neuilly-sur-Seine (1988).

(20) Schra, L., Ottens, H.H. and Vlieger, H., Fatigue crack growth in simulated Fokker 100 lap joints under MSD and SSD conditions, NLR Contract Report CR 95279 C, National Aerospace Laboratory, Amsterdam, June 1995.

(21) Vlieger, H. and Ottens, H.H., Results of uniaxial and biaxial tests on riveted fuselage lap joints specimens, NLR Contract Report CR 97319 L, National Aerospace Laboratory, Amsterdam, April 1997.

(22) De Jong, G.J., Elbertsen, G.A., Hersbach, H.J.C., and Van der Hoeven, W., Development of a full-scale fuselage panel test methodology, NLR Contract Report CR 95361 C, National Aerospace Laboratory, Amsterdam, May 1995.

(23) Vercammen, R.W.A. and Ottens, H.H., Full-scale fuselage panel tests, NLR Technical Publication TP 98148, National Aerospace Laboratory, Amsterdam, March 1998.

(24) Schijve, J., Fatigue life until small cracks in aircraft structures. Durability and damage tolerance, FAA/NASA International Symposium on Advanced Structural Integrity Methods for Airframe Durability and Damage Tolerance, NASA Conference Publication 3274, Editor C.E. Harris, Part 2, pp. 665-681, Hampton, Virginia (1994).

Table 1 Service or test histories of the pressure cabins

Aircraft type		Flights	Flight hours	Simulated flights
F28 – 4000	(1)	43,870	28,694	
	(2)	43,323	unknown	
F100				126,250 @ 110 % design load
BAC 1-11		75,158	52,000	
B 747-400				60,000 @ 100 % design load
B 727-100		53,424	59,848	
F28-1000		34,470	unknown	

Table 2 Estimates of MSD fatigue initiation lives in fuselage longitudinal lap splices

Aircraft type	MSD rivet row	Lives to first crack initiation	
		Flights	Simulated flights
F28-4000	outer sheet upper row	a few thousand?	
F100	outer sheet upper row		60,000 } @ 110 % design load
	inner sheet lower row		70,000 }
BAC 1-11	outer sheet upper row	60,000	
B 747-400	inner sheet lower row	50,000	
	outer sheet upper row		5,000–15,000 @ 100 % design load

D070-01N

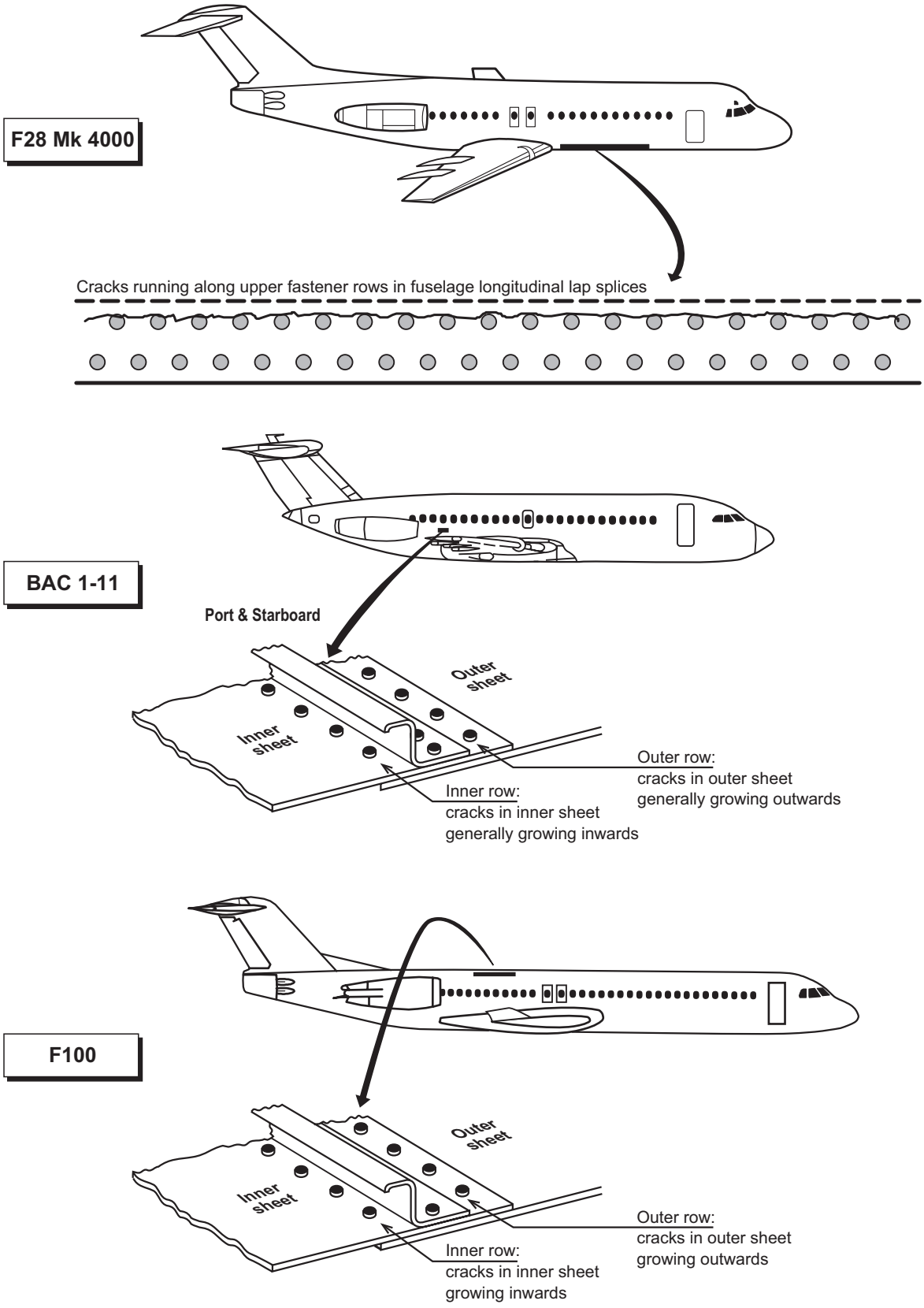

Fig. 1 Positions of the MSD fatigue cracked lap splices investigated by the NLR

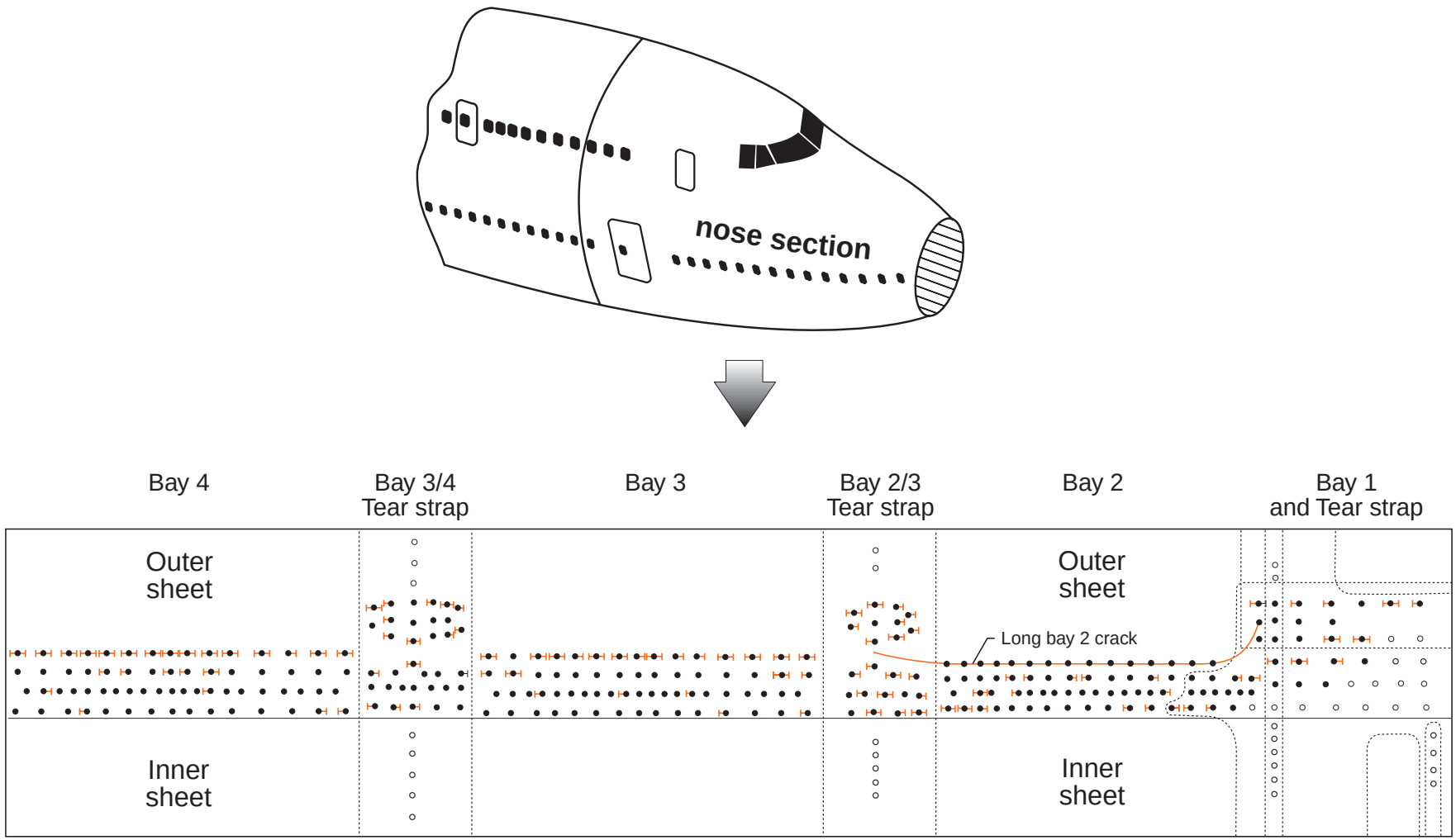

Fig. 2 Positions of the MSD fatigue cracks in the B 747-400 lap splice investigated by NASA [1]

D070-01N

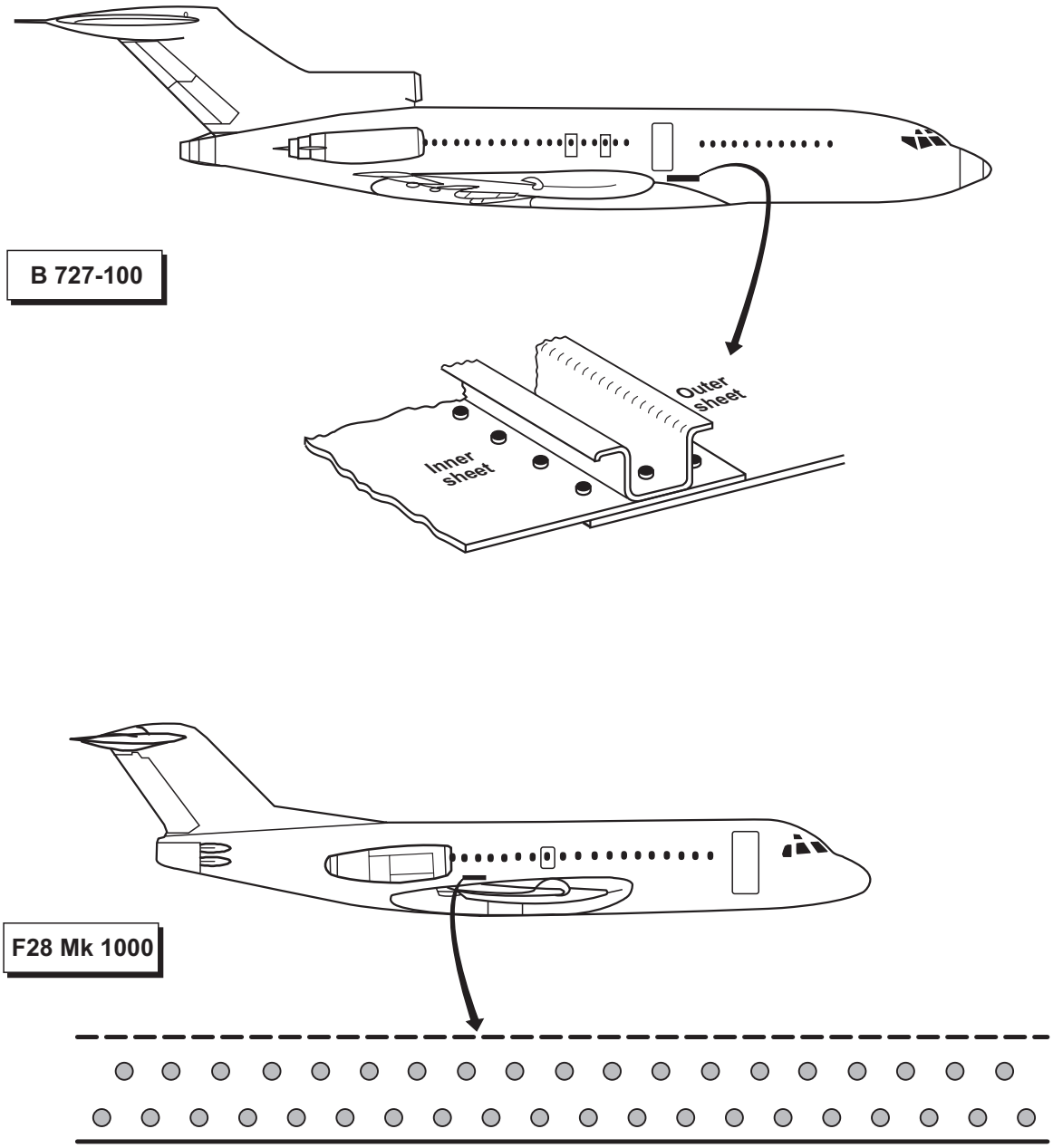

Fig. 3 Positions of the corroded lap splices

F28 Mk1000 & 4000

- **rivet pitch 16.6 mm**
- **rivet diameter 4 mm**
- **sheets chromic acid anodised and primed**

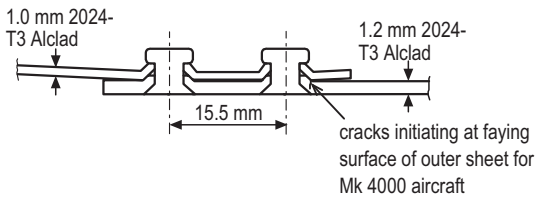

F100

- **rivet pitch 20 mm**
- **rivet diameter 3.2 mm**
- **sheets chromic acid anodised, primed and cold bonded**

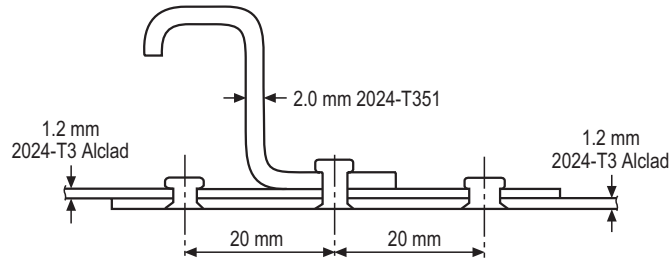

BAC 1-11

- **stiffener rivet pitch 12.7 mm**
- **sheet rivet pitch 25.4 mm**
- **rivet diameter 3.2 mm**
- **sheets chromic acid anodised and primed**
- **interfay sealant**

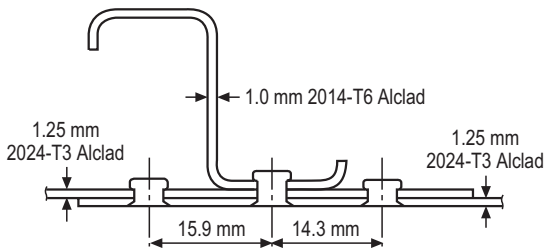

B 727-100

- **rivet pitch 28-30 mm**
- **rivet diameter 4.9-5.1 mm**
- **sheets and stiffener primed**
- **interfay sealant**

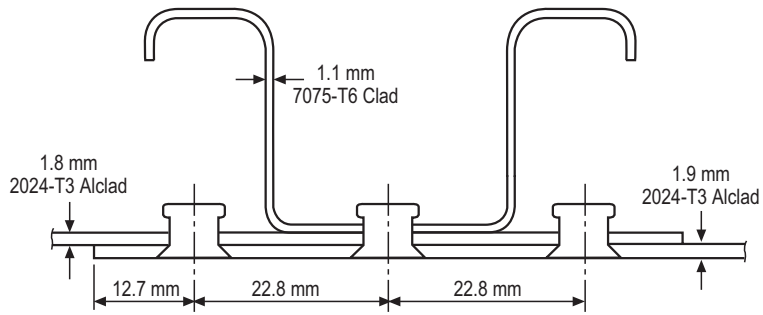

Fig. 4 Configurations of the lap splices investigated by the NLR, looking FORWARD

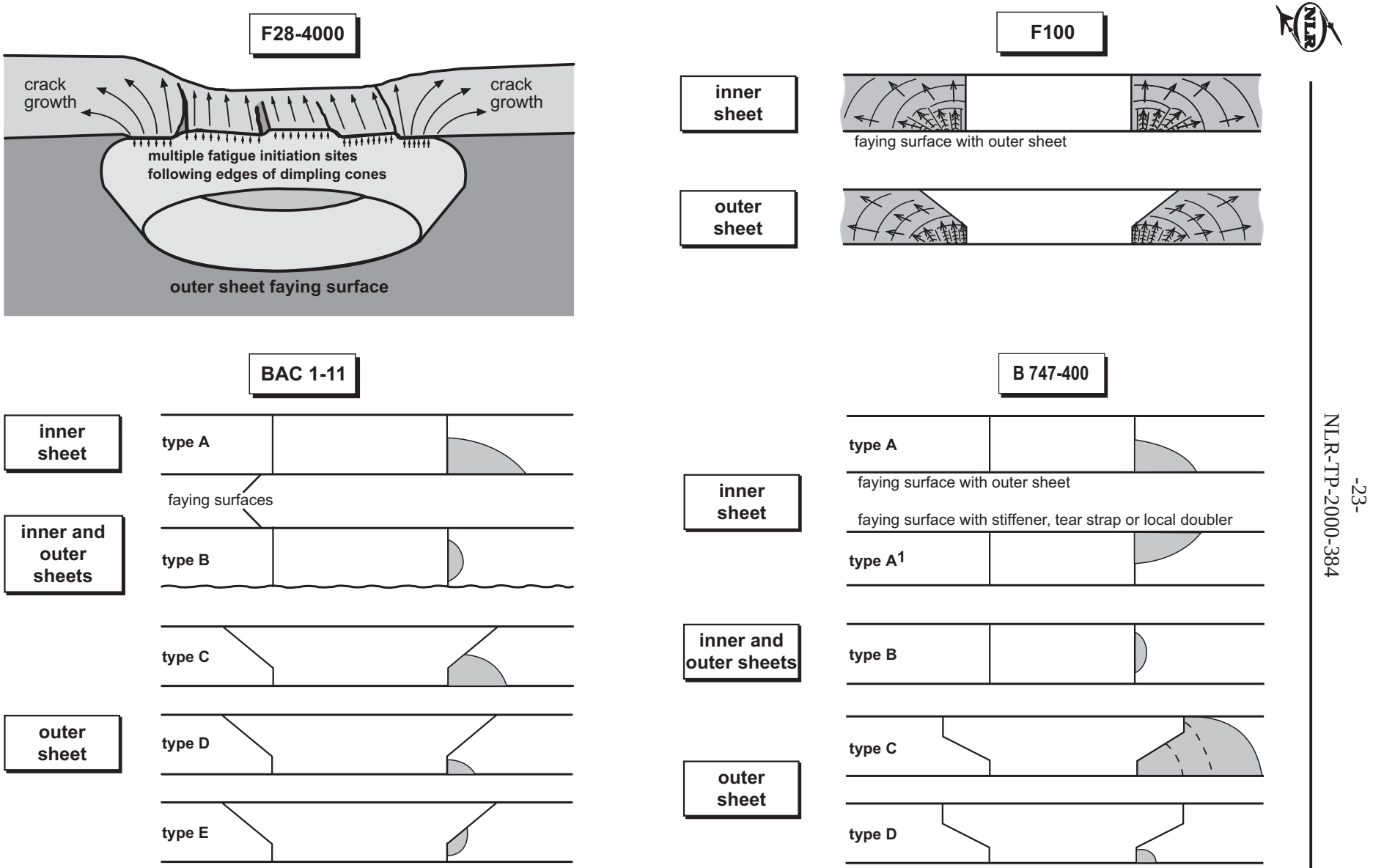

Fig. 5 MSD fatigue crack locations and shapes

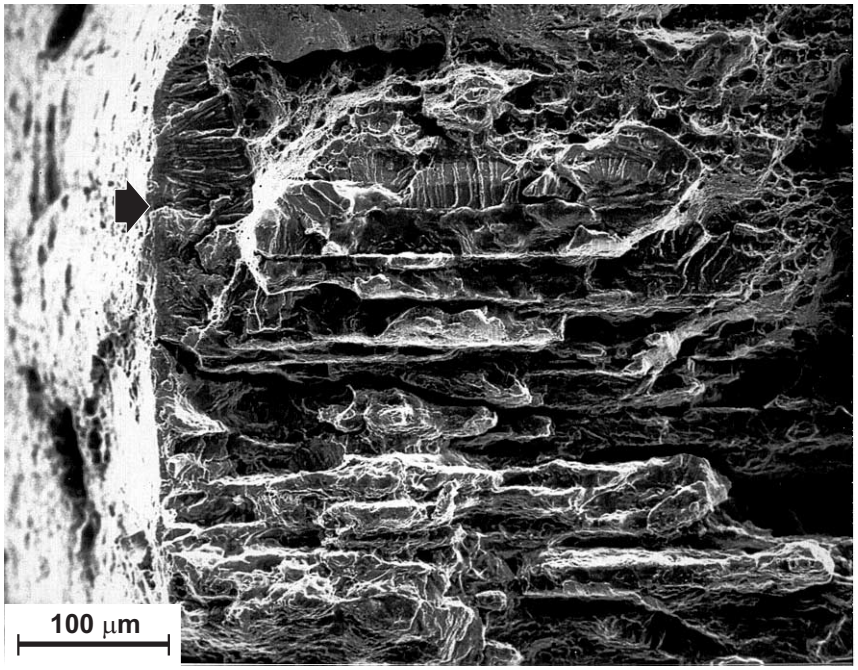

Fig. 6 Intergranular corrosion cracking (exfoliation and stress corrosion) with a secondary fatigue crack initiating from a rivet hole: B 727-100 lap splice outer sheet. The arrow points to the fatigue origin

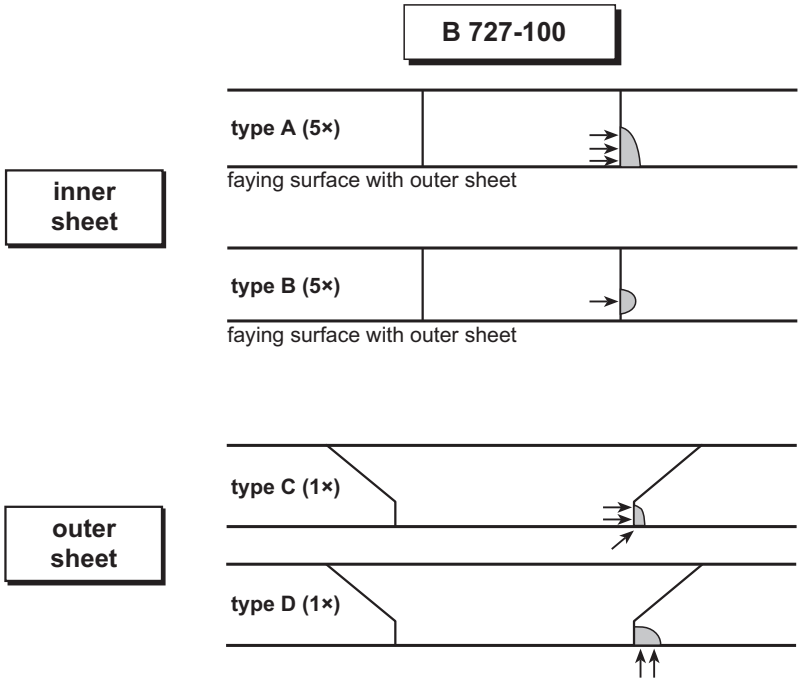

Fig. 7 Secondary fatigue cracks at or near rivet holes for the B 727-100 lap splice

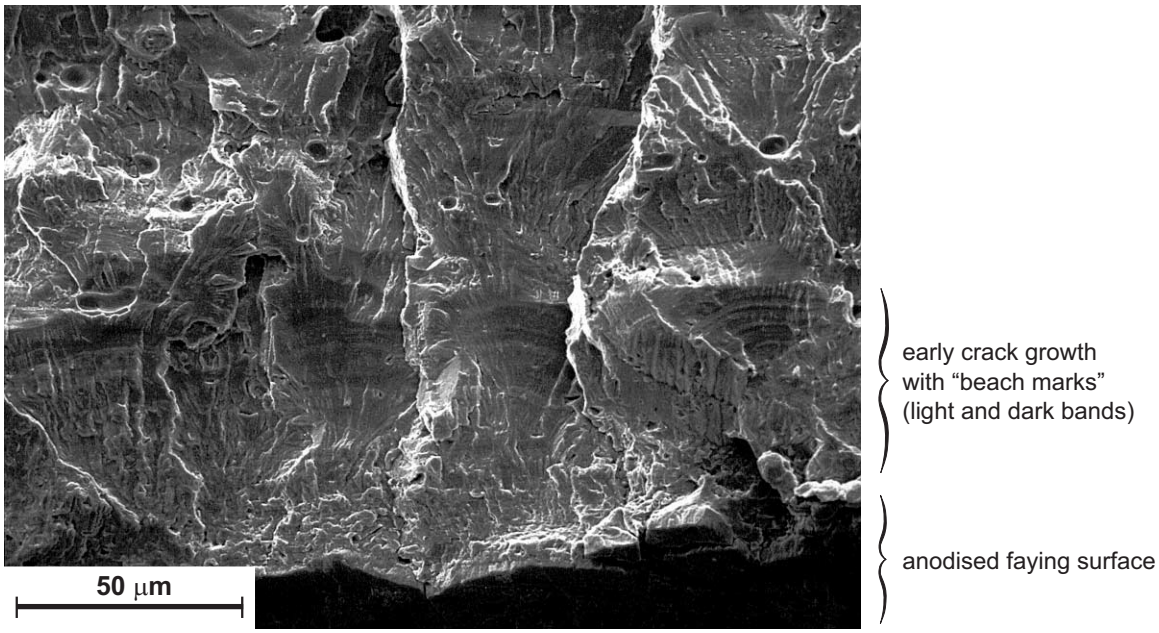

Fig. 8 Multiple site MSD fatigue initiation and early crack growth in an F28-4000 lap splice

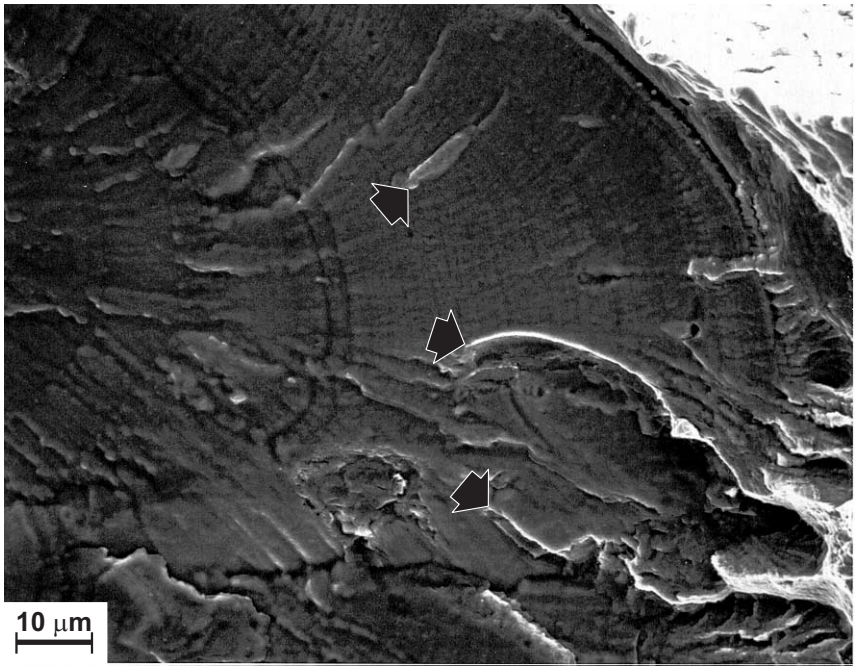

Fig. 9 Secondary fatigue crack early growth in the B 727-100 lap splice. Arrows point to narrow elliptical and semi-elliptical features with major axes in the local crack growth direction

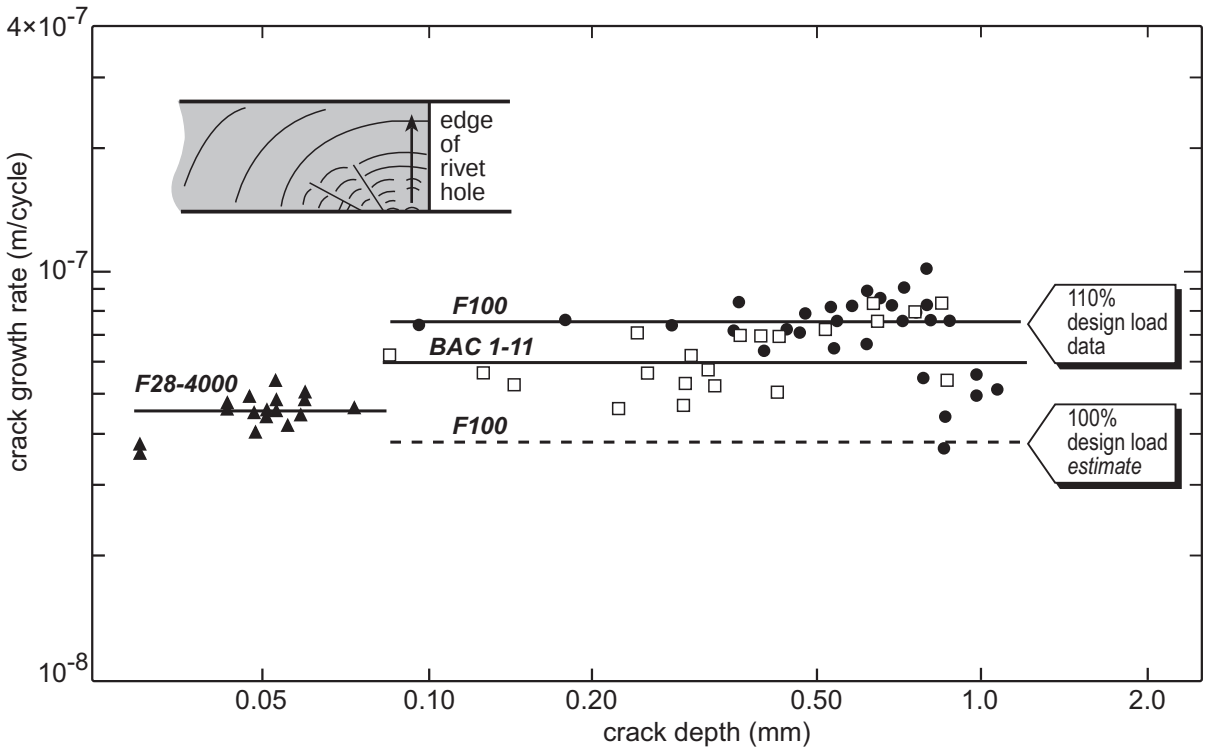

Fig. 10 Summary of transverse (through-thickness) fatigue crack growth rates

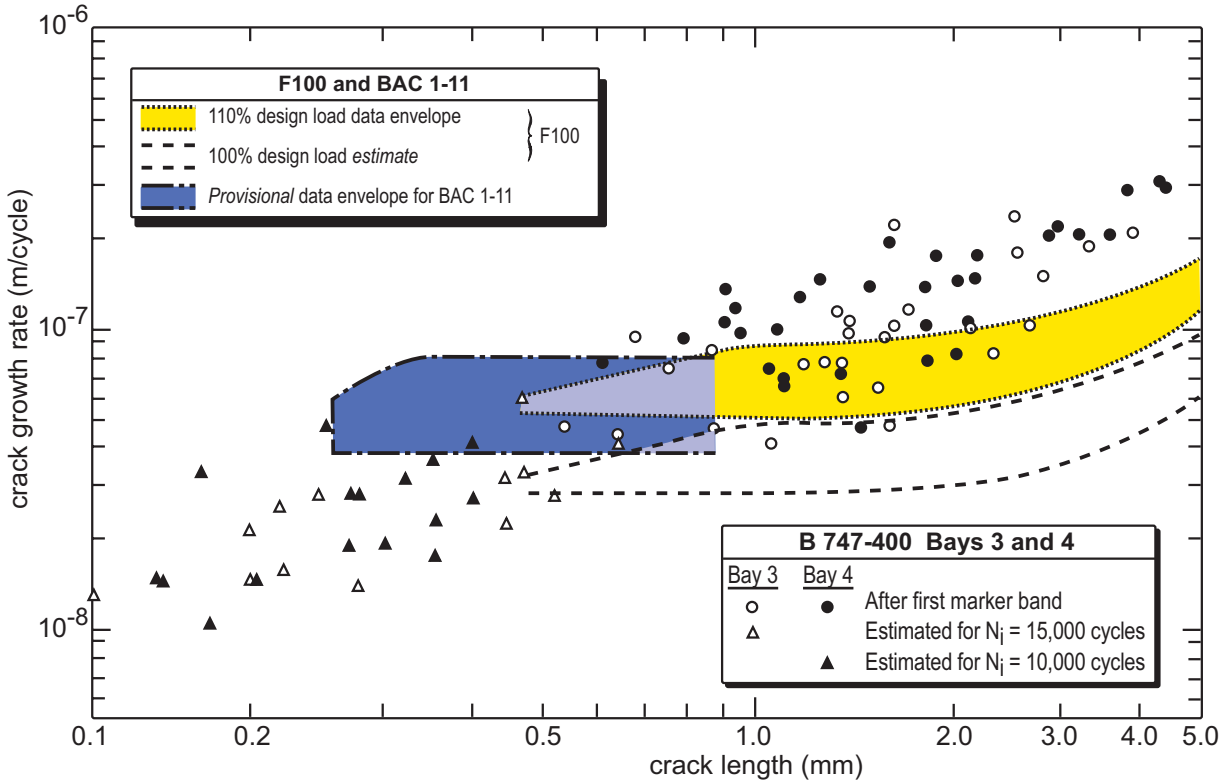

Fig. 11 Summary of longitudinal fatigue crack growth rates: B 747-400 data from NASA [1]

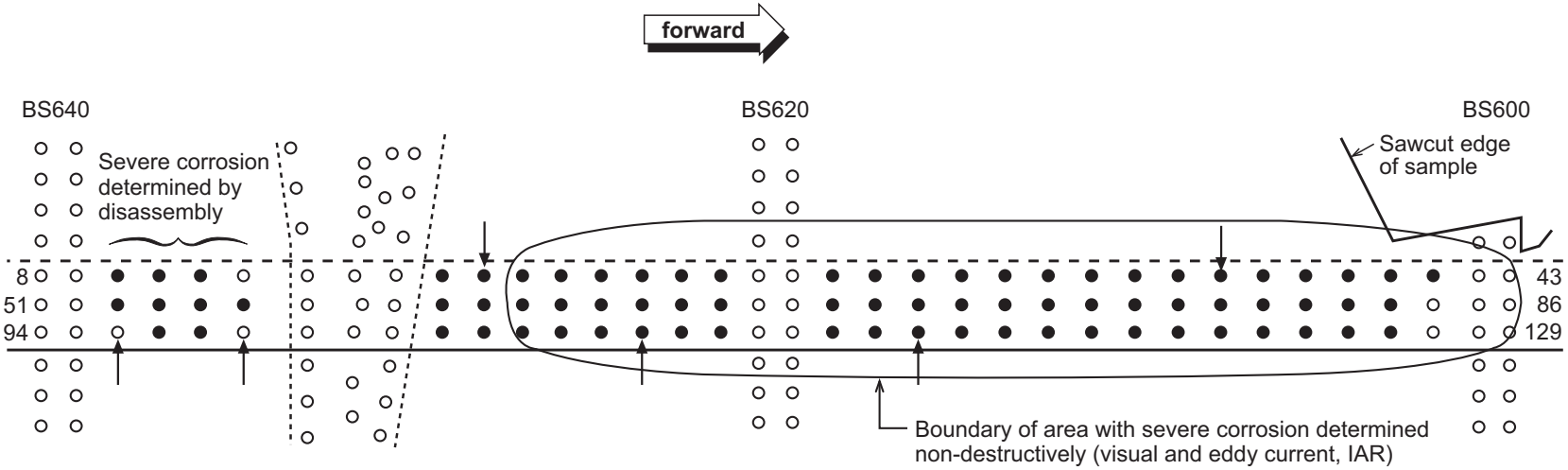

Fig. 12 Schematic of the results of the B 727-100 lap splice disassembly: ● = intergranular cracks; ↑ = fatigue cracks at rivet holes; BS = Body Station. The numbers at the ends of the rivet rows refer to the rivet positions.

- **From fractographic observations and striation spacings:**

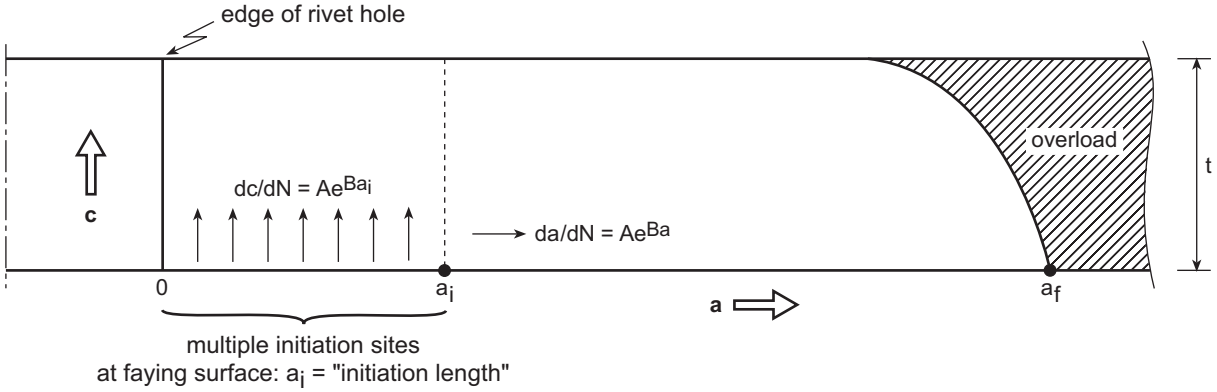

- **a_i, a_f and N_f are known. Calculate N_i from:** $N_f - N_i = \frac{1}{AB}\left(e^{-Ba_i} - e^{-Ba_f}\right)$
- **Calculate intermediate values of a for given values of n:** $a_{int} = -\frac{1}{B}\ln\left[e^{-Ba_i} - AB(N_{int} - N_i)\right]$
- **For each a_{int} calculate c_{int} from:** $c_{int} = (N_{int} - N_i)\,Ae^{Ba_i}$
- **Construct crack fronts as follows:**

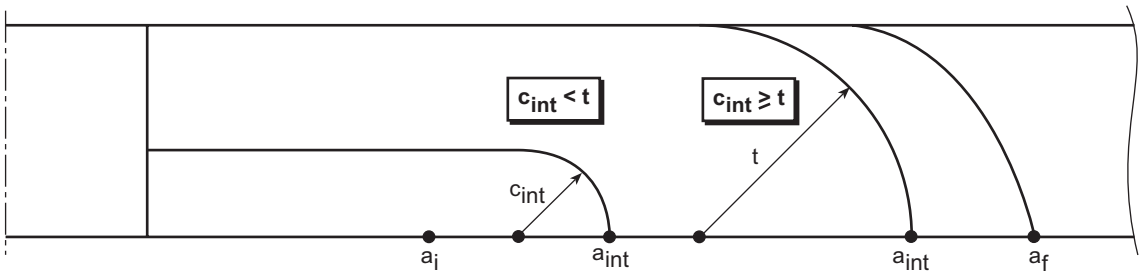

Fig. 13 Eijkhout's model illustrated for a non-countersunk sheet and multiple fatigue initiation sites

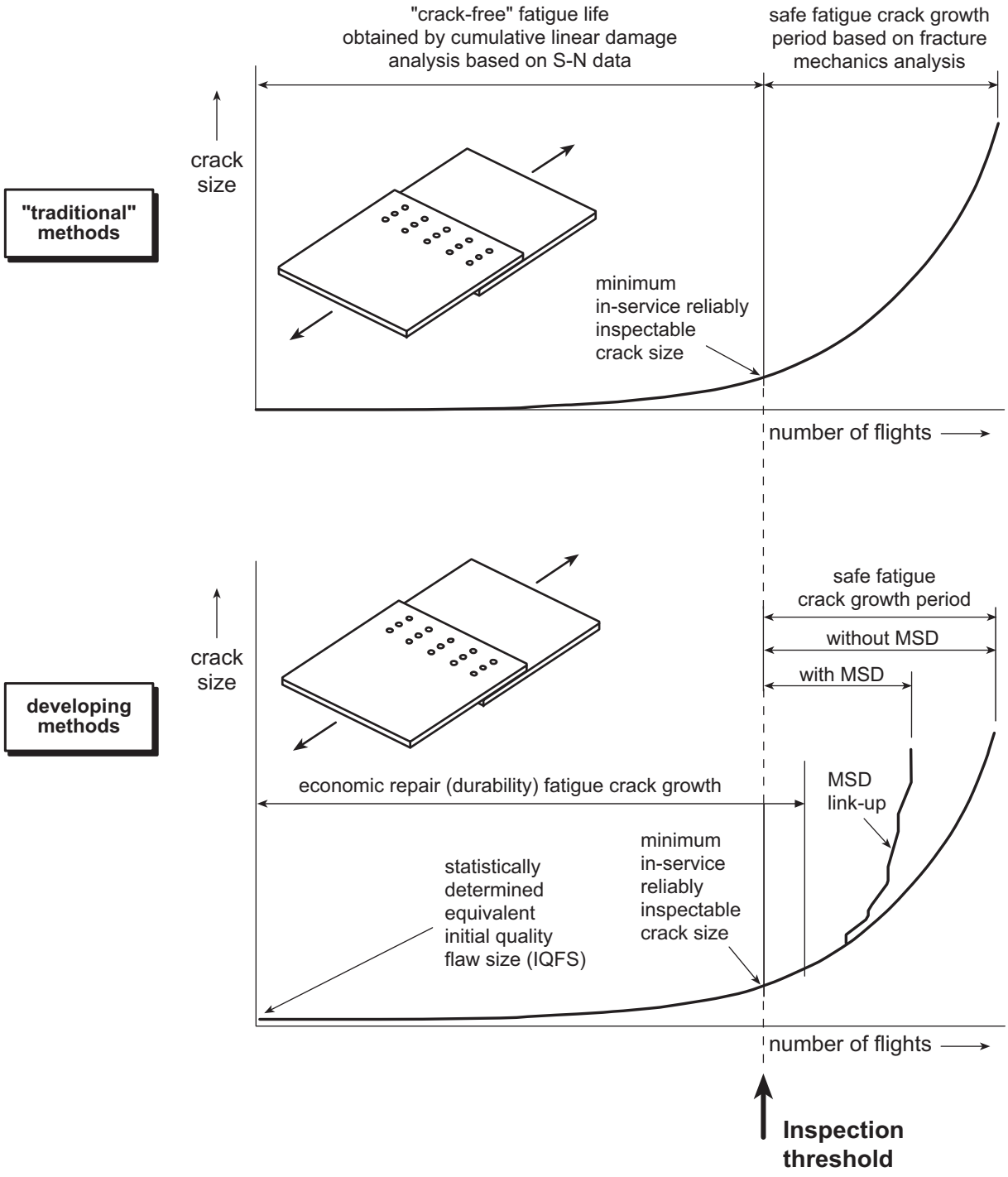

Fig. 14 Fatigue analyses for transport aircraft pressure cabin lap splices

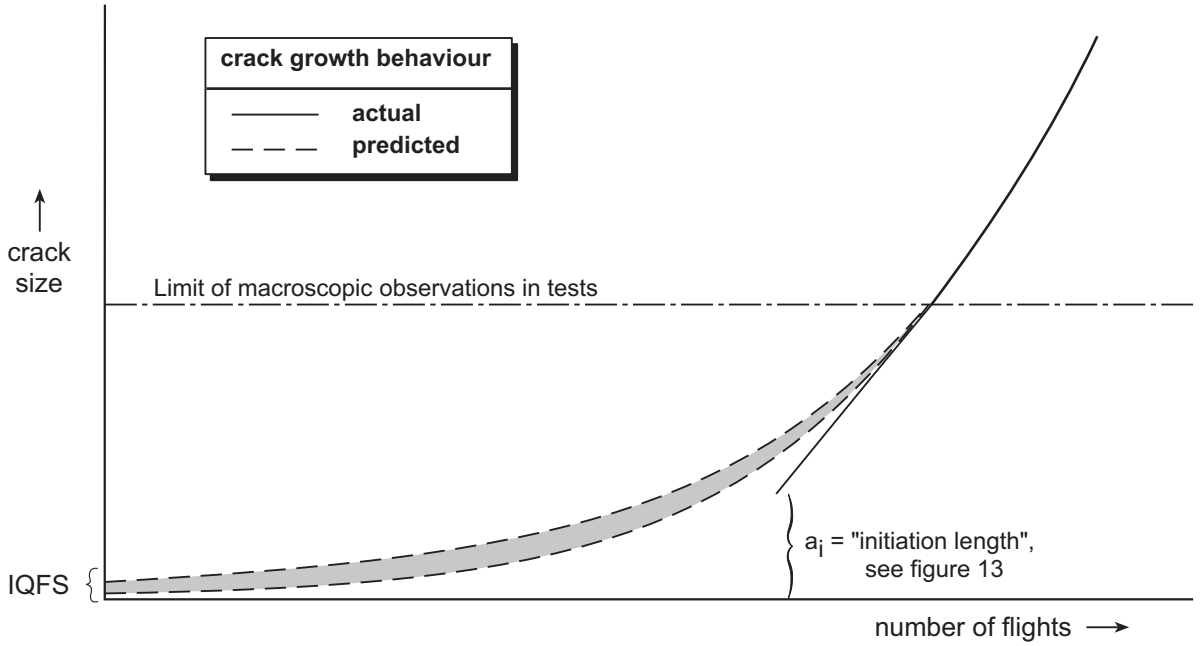

Fig. 15 Schematic differences between actual and predicted early MSD fatigue crack growth behaviour in transport aircraft pressure cabin longitudinal lap splices: the predictions are fitted to the macroscopic observations and the IQFS values are obtained from actual manufacturing flaws or by back-extrapolation using a macroscopic (long) crack growth model